Arch. Metall. Mater. **63** (2018), 4, 1749-1753

DOI: 10.24425/amm.2018.125101

E. ROCHA-RANGEL*#, J. LÓPEZ-HERNÁNDEZ*, J.A. CASTILLO-MARTÍNEZ*, J.J. OSORIO-RAMOS**,
C.A. CALLES-ARRIAGA*, I. ESTRADA-GUEL***, R. MARTÍNEZ-SÁNCHEZ***

STRUCTURE, MORPHOLOGY AND ELECTRICAL PROPERTIES OF $CaTiO_3$ CERAMICS SYNTHESIZED BY THE SOLID-STATE REACTION METHOD

In this paper, explain the preparation of $CaTiO_3$ ceramics synthesized by the solid-state reaction method. Calcium carbonate and titanium dioxide were high energy mixed in stoichiometric amounts, and the obtained mixture was calcined at different temperatures (800, 900, 1000 and 1300ºC) for 2 h. The obtained samples were characterized by measurement of particle size, Energy Dispersive X-Ray (EDX) Analysis; differential thermal analysis, X-ray diffraction and SEM images. XRD patterns indicated that $CaTiO_3$ ceramics with the structure of perovskite is obtained from calcined powders at 1,300°C for 2 h. SEM images show the formation of a very fine and homogeneous morphology. The measured values of electrical resistivity were within the typical range of insulating materials and approach values corresponding to insulating ceramics.

Keywords: $CaTiO_3$, Solid state synthesis, Electrical properties, Insulating ceramics

1. Introduction

Electroceramics are materials of high technological importance in which properties and applications depend on a complex interrelation between microstructure, processing, and chemical composition [1]. Depending on the electroceramic property of interest either mechanical, optical, magnetic and mainly electric, will be the type of control that must be taken in each variable during its processing. In addition, there is an increasing demand for high dielectric constant ceramics due to actual applications in microelectronics industry. The use of high dielectric constant materials allows the miniaturization of microelectronics structures [2]. A clear example of this situation is presented in ceramic varistors, materials that are characterized by not obeying Ohm's Law [1]. The ceramic varistors are often made of zinc oxide, which is doped with other metallic oxides of bismuth, cobalt, manganese, chromium, and antimony [3]. These oxides segregate towards the grain boundaries of the zinc oxide matrix, thereby generating the known Schottky barriers [4-6], which cause the non-linear behavior of the current-voltage (I-V) curve. For these reasons, the varistors are devices that can prevent electric surges and therefore are used in different electronic applications for the protection of equipment. Recently, compounds with the perovskite structure (ABO_3) and its derivatives, have been extensively studied due to their different physical properties and the high potential for technological applications [1,7-9]. Their electrical properties among others, allow them to be employed as varistors in electronic devices.

Calcium titanate ($CaTiO_3$) is a perovskite with cubic structure that has a high dielectric constant ($\varepsilon = 105$) at low frequencies, high melting point 1,975°C and therefore good thermal stability [1]. These characteristics make this material a potential candidate for diverse applications in the electronics industry [10]. However, as in any electroceramic compound, some deficiencies must be overcome, such as the strong dependence of the dielectric properties of the material with the processing route [11,12].

Usually, the perovskite of $CaTiO_3$ is obtained by solid state reactions of the precursor oxides ($CaCO_3$ y TiO_2), involving high temperatures and long sintering times, situations that significantly can affect the microstructure and therefore dielectric properties of the material. Besides, during heating there is the possibility of forming secondary phases [13]. There are other methods to prepare the $CaTiO_3$. Among them are wet chemical routes such as sol-gel, co-precipitation, self-combustion, microwave heating technique and microwave-assisted hydrothermal synthesis [1,14-25]. Although some of these methods have advantages such as the control of the chemical composition of the product, the costs are usually very high due to the high costs of precursor agents in addition to the complexity of the experimental method which makes them less productive processes.

Therefore, in the present paper, we investigate the electrical properties of $CaTiO_3$ ceramics synthesized by the solid-state reaction method. This approach is used to obtain compounds with fine and homogeneous microstructures that will be correlated with their dielectric properties.

* UNIVERSIDAD POLITÉCNICA DE VICTORIA, CIUDAD VICTORIA, AV. NUEVAS TECNOLOGÍAS5902, PARQUE CIENTÍFICO Y TECNOLÓGICO DE TAMAULIPAS, MÉXICO
** UNIVERSIDAD AUTÓNOMA METROPOLITANA, CDMX, MÉXICO
*** CIMAV, CHIHUAHUA, MÉXICO

Corresponding author: erochar@upv.edu.mx

2. Experimental details

For the present study, the $CaTiO_3$ perovskite was synthesized. For this purpose, a mixture in stoichiometric amounts in agreement with reaction (1) was prepared.

$$CaCO_{3(s)} + TiO_{2(s)} \xrightarrow{\Delta} CaTiO_{3(s)} + CO_{2(g)} \quad (1)$$

Powders of $CaCO_3$ (Sigma-Aldrich, 99.9% purity and 1 μm size) and TiO_2 (Sigma-Aldrich, 99.9% purity and 1 μm size) were milled in a planetary mill (Retsch PM 100) for 3 hours at a rotation speed of 300 rpm. A stainless steel container with zirconia grinding elements of 0.3 cm diameter was utilized as well as a powder weight/ball weight ratio of 1:12; no control agent was used during the milling. After milling the particle size distribution and specific surface area were determined using a Mastersizer 2000 equipment. Observations of milled powders and microstructure of sintered samples were performed by scanning electron microscopy (JEOL, JSM 6300). EDX spectrum was carried out with the intention of determining the chemical elements present in the sample. The mixtures of powders resulting from the milling step were subjected to a thermal at 800, 900, 1,000 and 1,300°C. This calcination was done in order to promote solid state chemical reaction between the particles as indicated by reaction (1). The thermal was carried out in an electric resistance furnace (Carbolite RHF17/3E) for 2 hours with an interval in each hour to grind the powder in a mortar and thus increase its surface area. The heating speed was 25°C/min. The progress of the chemical reaction was followed by thermogravimetric analysis (TA Instrument SDT Q600 V20.9) in addition to X-ray diffraction analysis (Siemens, D-5000). Resistivity and dielectric constant measurements were performed at 0 Hz frequency (direct current) at room temperature, using the 4-point method, applying currents of the order of nanoampers, through a controlled current source manufactured in our laboratories. This source was manufactured using circuits for stabilization of junctions in bipolar transistors [26].

3. Results and discussion

3.1. Powder size

In Fig. 1. The results of the particle size distribution are reported. This figure shows that for the $CaCO_3$ – TiO_2 powder mixture after the milling period, approximately 60% of the powders have particle sizes under 20 microns; about 30% of particles present 20 to 60 microns in size; and the remaining 10% of powders have sizes larger than 60 microns. These big sizes are due to the agglomeration of very small powders. The particle size is significant because the smaller they are, there will be a larger number of points of contact between the particles, situation which benefits the chemical reaction between $CaCO_3$ and TiO_2 reactants during the calcination step, thereby favoring the formation of the desired compound. The specific surface area that was obtained in the powder mixture was 11.6 m^2/g, which is a good indication that there is sufficient area of contact between the particles to carry out the reaction (1).

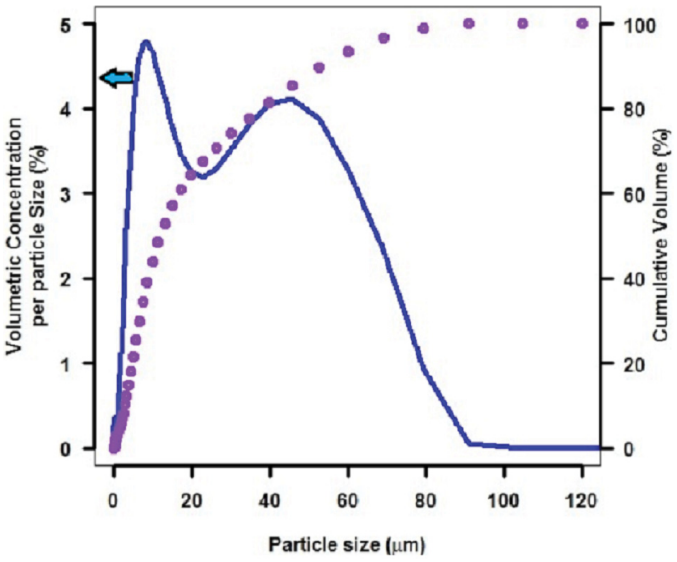

Fig. 1. Particle size distribution after milling stage

3.2. Powder composition

A micrograph of the powders after the grinding step is shown in Fig. 2. It shows the zone in which an analysis by EDX was carried out with the intention of determining the chemical elements present in the sample. In the EDX spectrum, the presence of Ca, Ti, C and O, chemical elements corresponding to the starting reactants ($CaCO_3$ and TiO_2) can be observed. Likewise, no other chemical elements are observed in the spectrum. Moreover, in this figure, the agglomeration of the powder, its round morphology and its very small size is appreciated.

3.3. Thermogravimetric analysis

Fig. 3. presents the curve of the thermogravimetric analysis for reaction (1). In this curve, a slight loss in weight is observed from room temperature to about 400°C. This is associated with the moisture evaporation absorbed by the sample during its milling. Subsequently, from 540°C, the loss in weight becomes considerable. This decline in weight ends near 660°C and is related to the decomposition of $CaCO_3$ and the consequent release of CO_2. The total loss weight of the sample due to both, moisture evaporation and CO_2 released was estimated in 7.52%. At higher temperatures the formation of $CaTiO_3$ perovskite must occur; however, because this reaction is not accompanied by a change in weight, it is not observable in this type of analysis. At 650°C, both the CaO and the TiO_2 are already available and will react at higher temperatures to form the desired $CaTiO_3$ perovskite. According to thermodynamic data the formation of $CaTiO_3$ has to occur at 970°C [27].

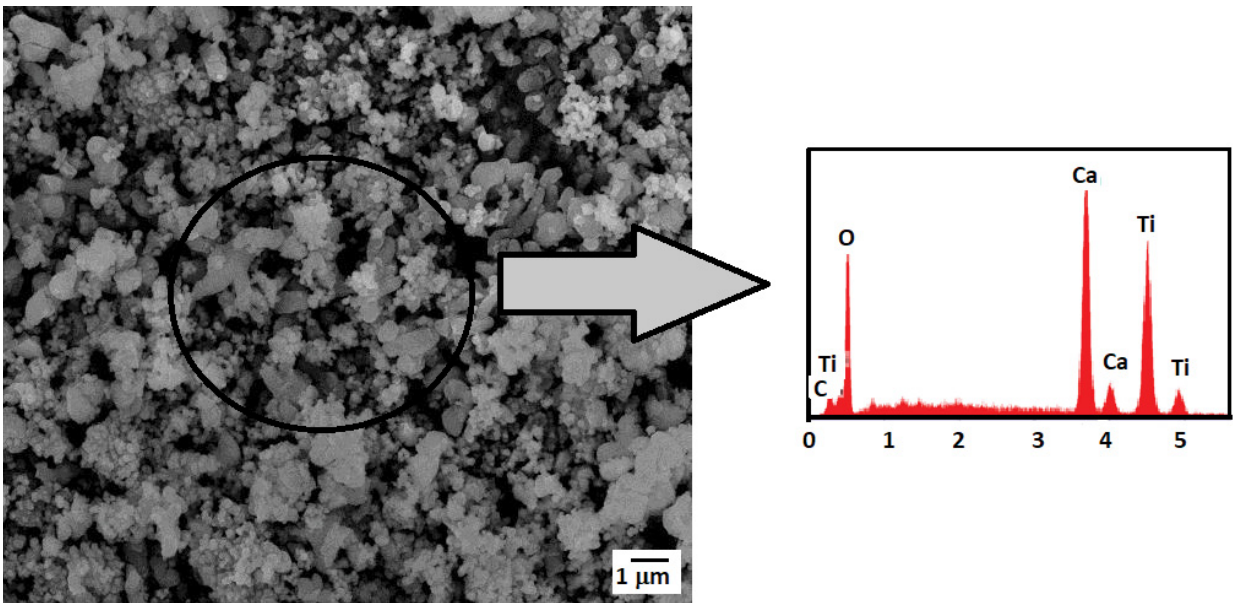

Fig. 2. EDX analysis performed in ground powders

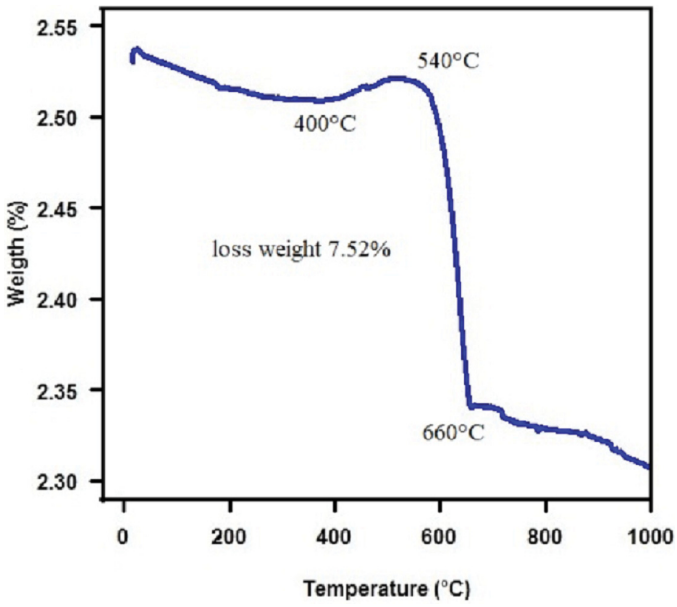

Fig. 3. Thermogravimetric analysis of reaction (1)

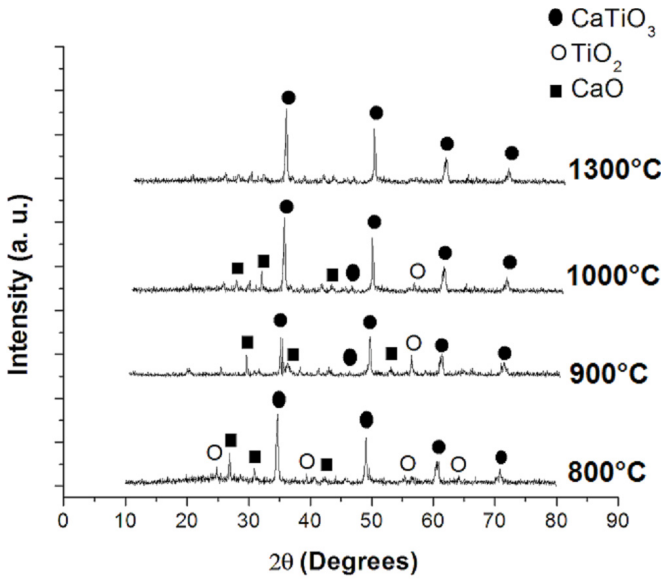

Fig. 4. X-ray diffraction patterns of $CaCO_3$ and TiO_2 powders calcined at different temperatures

3.4. X-ray diffraction

Fig. 4. shows the diffraction patterns obtained in powders of reaction (1) treated at different temperatures. It this figure it is observed that $CaTiO_3$ compound has reflection peaks at 34.8, 46.3, 47.9, 61.4 and 72.1° which correspond to the planes (110), (200), (210), (211) and (220) respectively. Meanwhile, the XRD spectrum for TiO_2 displays reflection peaks at 24.8, 38.2, 56.8 and 63.4°, related to the planes (101), (004), (105) and (204) and which correspond to the anatase structure of TiO_2. Finally, there are reflection peaks in 27.2, 31.4, 36.7, 43.5 and 53.2°, which correspond to the (012), (013), (200), (015) and (220) planes of CaO. In some reflection peaks there are small deviations in the angle 2θ. This behavior is due to the modification of the lattice parameter due to high deformation of the crystal structure during the milling stage. The high intensity at 34.8°, 2θ indicates that the $CaTiO_3$ crystals grow along the preferential direction (110).

From the XRD results, it can be concluded that as the temperature increases, the corresponding peaks of CaO and TiO_2 decrease in intensity, while the intensity of $CaTiO_3$ perovskite peaks increases. The figure shows that at 1,000°C the chemical reaction (1) has been completed, and only traces of the initial reagents remain. The original $CaCO_3$ carbonate is not observed in these diffraction patterns, since $CaCO_3$ in agreement with the TGA analysis, decomposes entirely at 650°C. In addition, the tests shown here were performed on samples treated at 800, 900, 1,000 and 1300°C.

The crystallite size for sample calcined at 1300°C was calculated by using the Debye-Scherrer equation (2) [28]:

$$D = \frac{0.9_{k\alpha}}{B_{2\theta}\cos\theta} \quad (2)$$

Where D is the crystallite size, 0.9 is the shape factors for spherical particles, λ the radiation wavelength (1.5406A), $B_{2\theta}$ is the full width at half maximum, and θ is the Bragg diffraction angle for each crystalline plane. The calculated value for the $CaTiO_3$ crystal size was 85.8 nm.

3.5. Morphology

SEM observation of the morphology of $CaTiO_3$ perovskite calcined at 1,000°C is presented in Fig. 5. In this figure grains with polymorphic but homogeneous shapes are observed; the grain size is in the order of nanometers. This observation is in agreement with the calculus of particles size performed with the information of the XRD analysis which gives a value of 85.8 nanometers. In general, it can be said that the morphology presented by the perovskite manufactured through the proposed methodology presents very small powder sizes with polymorphic shape which causes the formation of a large number of contacts between grains. This situation evidently favors the resulting low values of resistivity in this compound.

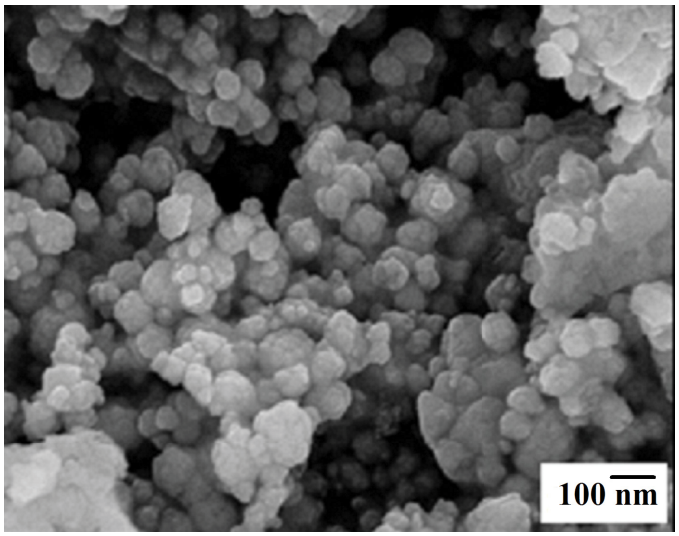

Fig. 5. Morphology of $CaTiO_3$ perovskite calcined at 1,000°C

3.6. Electrical properties

In Table 1, the electrical resistivity and conductivity values of the calcined materials are reported as a function of the calcination temperature. As can be seen in this table, as the calcination temperature increases, the resistivity of the material also increases. This situation is associated with the progress of chemical reaction (1). According to the results of XRD, at 1,000°C we have the formation of $CaTiO_3$ perovskite, at temperatures of 800 and 900°C although the presence of $CaTiO_3$ is already present, CaO and TiO_2 are also present in the material, and therefore the latter compounds must be acting as dopants of $CaTiO_3$ perovskite causing its resistivity to be slightly lower. The resistivity values presented by all the samples obtained here are within a range characteristic of insulating materials, typically from 10^8 to 10^{20} Wm [28]. The low resistivity values of these materials are due to the high concentration of flaws in the samples, which were probably introduced into them during the high intensity grinding to which the original powders were subjected.

Also in table 1, the dielectric constant of processing materials is presented. In this table, it can be seen that after the calcination step at different temperatures, samples have different values of the dielectric constant. A linear behavior of this property with the temperature is not observed as it happens in the results of the electrical resistivity. This strange behavior of the dielectric constant is probably due to the presence of secondary phases like CaO and TiO_2 in the calcined samples.

TABLE 1

Estimated resistivity, conductivity and dielectric constant of studied perovskite $CaTiO_3$

Synthesis temperature (°C)	Conductivity (Sm^{-1})	Resistivity (Wm)	Dielectric constant
800	6.3025×10^{-11}	1.5866×10^{10}	47.8828
900	5.7773×10^{-11}	1.7309×10^{10}	69.4966
1,000	5.2521×10^{-11}	1.904×10^{10}	39.9024

4. Conclusions

In summary, pure $CaTiO_3$ ceramics perovskite-type with orthorhombic structure was synthetized by solid state reaction at 1,300°C for 2 h as proved by X-ray analysis. SEM images showed the presence of fine and very small grain sizes through the proposed methodology. Moreover, the polymorphic shape which causes the formation of a large number of grain boundaries, a situation that favors the obtaining of low values of resistivity in this oxide. Our electrical measurements indicate that this kind of perovskites has very low electrical conductivity making them suitable for electronic applications, such as protector of electric shocks in electronic gadgets. The high dielectric constant and isolation capability presented by the $CaTiO_3$ ceramics make it suitable for capacitors miniaturization.

Acknowledgements

The laboratories facility given by UPV, UAM-A, and CIMAV is appreciated. Besides, ERR is grateful to CONACyT by the support provided to carry out this work through Project 270294.

REFERENCES

[1] M.I. Ahmed, A. Habib, S.S. Javaid, Int. J. Photoenergy. **2015**, 1-13 (2015).

[2] S.J. Fiedziuszko, I.C. Hunter, T. Itoh, Y. Kobayashi, T. Nishikawa, S.N. Stitzer, K. Wakino, IEEE Trans. Microw. Theory Tech. **50** (3), 706-720 (2002).

[3] O. Martínez-Urgell, E. Rocha-Rangel, C. Gomez-Yánez, Adv. In. Tech. of Mat. and Mat. Proc. J. **9** (1), 87-90 2007.

[4] F. Gruter G. Blatter, Semicond. Sci. Technol. **5**, 110-11, (1990).

[5] M. Matsuoka, Jpn. J. Appl. Phys. **10**, 736-741 (1971).

[6] L.M. Levinson, H.R. Philipp, Am. Ceram. Soc. Bull. **65**, 639-641 (1986).

[7] M. Dawber K.M. Rabe, J.F. Scott. Rev. Mod. Phys. 77 (4), 1083-1130 (2005).

[8] M.A. Green, A. Ho-Baillie, H.J. Snaith. Nature Photon. **8** (7), 506-514 (2014).

[9] M.L. Moreira, E.C. Paris, G.S. Do Nascimento, V.M. Longo, J.R. Sambrano, V.R. Mastelaro, M.I.B. Bernardi, J. Andres, J.A. Varela, E. Longo. Acta Mater. **57**, 5174-5185 (2009).

[10] M.A. Ramírez, A.Z. Simõesb, A.A. Felix, R. Tararam, E. Longo, J.A. Varela. J. Alloys Compd. **509** (41), 9930-9933 (2011).

[11] R. Kashyap, T. Dhawan, P. Gautam, O.P. Thakur, N.C. Mehra, R.P. Tandon. Mod. Phys. Lett. B. **24** (12), 1267-1273 (2010).

[12] T.B. Adams, D.C. Sinclair, A.R. West. J. Am. Ceram. Soc. **89**, 3129-3135 (2006).

[13] C.M. Wang, S.Y. Lin, K.S. Kao, Y.C. Chen, S.C. Weng. J. Alloys Compd. **491** (1-2), 423-430 (2009).

[14] A. Lopera, C. García, M. Ramírez, C. Paucar, J. Marín, D. Hotza. Revista Colombiana de Materiales. **5**, 269-276 (2014).

[15] F. Amaral, M. Valente, L.C. Costa. Mater. Chem. Phys. **124** (1), 580-586 (2011).

[16] M. Sahebali. and J. Mojtaba. Int. J. Phys. Sci. **8** (23), 1277-1283 (2013).

[17] Q. Zhang, X. Li, Z. Ren, G. Han, C. Eur. J. Inorg. Chem. **27**, 4532-4538 (2015).

[18] C.H. Jung, Y.K. Kim, Y.M. Han, S.J. Lee. J Nanosci Nanotechnol. **16** (2), 1676-1679 (2016).

[19] H. Chong, L. Jingjing, Y. Wangjin, W. Qianqian, Y. He, X. Xiangxin. J. Sol-Gel Sci. Technol. **3**, 145-149 (2017).

[20] G. Gralik, A.E. Thomsen, C.A. Morae, F. Raupp-Pereira, D. Hotza. Process. Appl. Ceram. **8** (2), 53-57 (2014).

[21] H.S. Kim, S.H. Im, N.G. Park. J. Phys. Chem C. **118** (11), 5615-5625 (2014).

[22] S.K. Manik, S.K. Pradhan, M. Pal. Physica E. **25**, 421-424, (2005).

[23] Q. Zhang, X. Li, Z Ren, G. Han, C. Mao. Eur J. Inog. Chem. **2015** (27), 4532-4538, (2015).

[24] B.M. Patil, R.S. Srinivasa, S.R. Dharwadkar. Bull. Mater. Sci. **30** (3), 225-229 (2007).

[25] X. Yang, J. Fu, C. Jin, J. Chen, C. Liang, M. Wu, W. Zhou, J. Am. Chem. Soc. **132** (40), 14279-14287 (2010).

[26] B.L. Hart, The Radio and Electronic Engineer, **50**, (1/2), 79-89 (1980).

[27] A.K. Galwey, M.E. Brown, Thermal decomposition of ionic solids, Elsevier, Amsterdam (1999).

[28] B.D. Cullity, S. R. Stock, Elements of X-Ray Diffraction, Prentice Hall, New Jersey (2001).

[29] X.A. Moulson, A. Herbert, Electroceramics: Materials, Properties, Applications, Wiley, New York (2003).